Supplemental Data

Nucleocytoplasmic Oscillations of the Yeast Transcription Factor Msn2: Evidence for Periodic PKA Activation

Cecilia Garmendia-Torres, Albert Goldbeter, and Michel Jacquet

Experimental Procedures

Yeast Strains and Growth Conditions

The following yeast strains were used: W303-1B (MATα, *ade2*, *ura3*, *his3*, *leu2*, *trp1*), Y3398 (MATα, *tpk1::HIS3*, *tpk2$^{w(Q138E)}$*, *tpk3::TRP1*, *bcy1::LEU2*, *ade2-1*, *can1-1000*, *his3-11,15*, *leu2-3,112*, *trp1-1*, *ura3-1*, *GAL*), Y3399 (MATα, *tpk1::HIS3*, *tpk2$^{w(E235Q)}$*, *tpk3::TRP1*, *bcy1::LEU2*, *ade2-1*, *can1-1000*, *his3-11,15*, *leu2-3,112*, *trp1-1*, *ura3-1 GAL*), F1D (*MATa*, *ade2*, *can 1-100*, *CRI4*, *his3*, *leu2-3,112*, *lys1-1*, *ura3-52*, *ras1::URA3*, *ras2::LEU2*) [S1], YNP2 (*MATa*, *pse1-1*, *kap123Δ*, *trp1−Δ63*, *leu2 Δ*, *ura3-52*), and PSY1201 (*MATa*, *pse1-1*, *trp1−Δ63*, *leu2 Δ*, *ura3-52*) [S1]. The *tpk^{w}* strains were gifts from J. Broach. The strains YNP2 and PSY1201 were gifts from P. Silver.

All of the cultures were performed at 30°C in YNB medium supplemented by the required amino acids.

Plasmid Constructions

In all of the constructions, we used pAMG as a template [S2], and the sequences of oligonucleotides we used are shown in Table S1.

An intermediary plasmid called pO1 was made in order to facilitate further constructions. This plasmid is derived from pAMG and contains the ATG, a small polylinker (SalI, BamHI, and PstI), and the sequence of *MSN2* from 1723 to the end and the sequence of GFP. The *MSN2-GFP* open reading frame (ORF), cut out by SalI and HindIII, has been replaced by the SalI-HindIII-cut polymerase chain reaction (PCR) fragment obtained by oligonucleotides ol1 up and olGFPh.

For the creation of pMsn2-ΔNter-GFP, a SalI-PstI-cut PCR fragment obtained from oligonucleotides ol2 up and ol2 down was inserted in the SalI-PstI-cut pO1. In the case of pMsn2-ΔNter-ΔZ-GFP, a SalI-NotI-cut PCR fragment obtained from oligonucleotides ol2 up and ol3 down was inserted in the SalI-NotI-cut pO1. For pMsn2-NES-PKI-GFP, oligos olPKI_Sal and olPKI_Pst were hybridized and cut by SalI and PstI to be cloned into pO1. For the creation of pMsn2-NLS-SV40, a PCR fragment was obtained from oligonucleotides olMsn2+1 up and ol Msn2+575NLS down, and it was inserted into the SalI-NotI-cut pO1.

The plasmid pMsn2-ΔZ-GFP is described as pAMG-ΔZ in Jacquet et al. [S3]. pGR213 was obtained from a SalI-cut fragment from pJL42 [S3] inserted into pUG34.

Time-Lapse Microscopy

Time-lapse microscopy was performed with the setup previously described [S3]. It consisted of an inverted microscope, Leica DM IRE2, that was mounted on an antivibration table and placed in an incubator (Life Imaging Services, the Cube) at constant temperature (30°C). The oil-immersion objective was a 100× HCX PL APO that was z positioned with a piezoelectric driver (LVPZ-T position servocontroller, Physik Instrumente GmbH). Fluorescence was recorded with a charge-coupled device (CCD) detector (Photometrics CoolSNAP HQ, Roper Scientifics). For illumination, we used a Xenon Lamp 75 W, ebx 75. The experimental setup was steered by Metamorph 6.2r6 Software (Universal Imaging).

Imaging

Every 10 s, during a 1 s period, a stack of 21 frames along the z axis (every 0.3 μm) was recorded (except for *tpk2^{W}* observations, which were recorded every 20 s during 2 s period). Images were deconvoluted as previously described [S3]. For each stack, a brightest-point z projection was done with the Metamorph program to obtain the final reconstructed image. Pixel values in the nucleus and the cytoplasm, after removal of background noise, were used to monitor the distribution of Msn2-GFP over time, with Image J software.

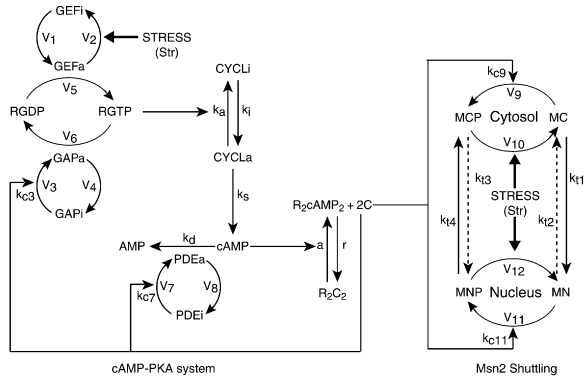

Figure S1. Model of the cAMP-PKA Pathway Coupled to Msn2 Subcellular Localization

The model is identical to that shown in Figure 2 in the main text, with indication of the parameters associated with each reaction step.

Model Predicting Oscillations of Msn2 through Oscillations of the cAMP-PKA Pathway

Model Predicting Oscillations of the cAMP-PKA Pathway

The variables of the model schematized in Figure 2 and Figure S1 are the following: the fractions GEFa and GAPa of active GEF and GAP proteins; the fraction RGTP of Ras protein bound to GTP; the fraction CYCLa of adenylate cyclase in the active state; the concentration cAMP of cyclic AMP; the fraction of active phosphodiesterase PDEa; and the fraction R_2C_2 of PKA in the form of a holoenzyme complex between the regulatory (R) and catalytic (C) subunits, free of cAMP. R_2cAMP_2 denotes the holoenzyme with a cAMP molecule bound to each of the two regulatory subunits. The time evolution of these variables is governed by the following set of kinetic equations:

$$\frac{dGEFa}{dt} = V_1\frac{(1-GEFa)}{K_1+(1-GEFa)} - V_2\frac{GEFa}{K_2+GEFa} \quad \text{(S1A)}$$

$$\frac{dGAPa}{dt} = V_3C\frac{(1-GAPa)}{K_3+(1-GAPa)} - V_4\frac{GAPa}{K_4+GAPa} \quad \text{(S1B)}$$

$$\frac{dRGTP}{dt} = V_5GEFa\frac{(1-RGTP)}{K_5+(1-RGTP)} - V_6GAPa\frac{RGTP}{K_6+RGTP} \quad \text{(S1C)}$$

$$\frac{dCYCLa}{dt} = k_a(RGTP)(RASt)(1-CYCLa) - k_iCYCLa \quad \text{(S1D)}$$

$$\frac{dPDEa}{dt} = V_7C\frac{(1-PDEa)}{K_7+(1-PDEa)} - V_8\frac{PDEa}{K_8+PDEa} \quad \text{(S1E)}$$

$$\frac{dcAMP}{dt} = k_s(CYCLa)(CYCLt) - k_d(PDEt)(PDEa)\frac{cAMP}{K_{md}+cAMP} - 2V_{PKAact}PKAt \quad \text{(S1F)}$$

$$\frac{dR_2C_2}{dt} = -a(R_2C_2)(cAMP)^2 + rC^2(R_2cAMP_2)(PKAt)^2 \quad \text{(S1G)}$$

where

$$V_1 = V_{max1}/\text{GEFt}, V_2 = Str.V_{max2}/\text{GEFt};$$

$$V_3 = k_{c3}\text{PKAt}/\text{GAPt}, V_4 = V_{max4}/\text{GAPt};$$

$$V_5 = k_{gef}\text{GEFt}/\text{RASt}, V_6 = k_{gap}\text{GAPt}/\text{RASt};$$

Table S1. List of Oligonucleotides

Name	Sequence
ol1 up	AACGCGTCGACGACGGATCCGACCTGCAGTCTTCCCTTCGGAGGCGGAAG
ol GFPh	CCCCAAGCTTTTACTTGTACAGCTCGTCCAT
ol2 up	AACGCGTCGACTGAACATAGACTCCATGCTA
ol2 down	TTTTCTGCAGAGAACCGATTTTAGAGTTCAT
ol3 dowm	AAATATGCGGCCGCCTTCCTTTGTTGATTCTATT
olPKI_Sal	ATGACGGTCGACAGCAATGAATTAGCCTTGAAATTAGCAGGTCTTGATATCAACAAGACACTGCAGCCAAGT
olPKI_Pst	ACTTGGCTGCAGTGTCTTGTTGATATCAAGACCTGCTAATTTCAAGGCTAATTCATTGCTGTCGACCGTCAT
ol Msn2+1	ACGCGTCGACCATGATTTCAAT
ol Msn2+575 NLS	ATAGTTTAGGTGCGGCCGCCAACCTTTCTCTTCTTCTTTGGAGAACCGATTTTAGAGTTCA

$V_7 = k_{c7}\mathrm{PKAt}/\mathrm{PDEt}, V_8 = V_{\max 8}/\mathrm{PDEt};$

$V_{PKAact} = a(R_2C_2)(cAMP)^2 - rC^2(R_2cAMP_2)(PKAt)^2$; and

$$\mathrm{R_2cAMP_2} = 1 - \mathrm{R_2C_2}, \mathrm{C} = 2(1 - \mathrm{R_2C_2}). \quad \text{(S2)}$$

In the above equations, GEFt, GAPt, RASt, CYCLt, PDEt, and PKAt denote, respectively, the total concentrations of the proteins GEF, GAP, RAS, adenylate cyclase, and PKA; cAMP denotes the cellular concentration of cAMP. The negative-feedback regulation by PKA is introduced in Equations S1B and S1E, with the assumption that the catalytic subunit C of PKA catalyzes the phosphorylation of the inactive GAP protein into the active form GAPa and also controls the activation of PDE. We assume that stress acts by reducing the maximum rate at which the enzyme inactivates GEF; Str represents the dimensionless parameter measuring stress intensity.

Coupling the Nucleocytoplasmic Shuttling of Msn2 to PKA

When taking into account the phosphorylation of Msn2 by PKA, the time evolution of the fractions of unphosphorylated and phosphorylated Msn2 in the cytosol (MC and MCP) and in the nucleus (MN and MNP) are governed by the following kinetic equations:

$$\frac{dMC}{dt} = -k_{t1}MC + k_{t2}MN - V_{11}C\frac{MC}{K_{11}+MC} + V_{12}\frac{MCP}{K_{12}+MCP} \quad \text{(S3A)}$$

$$\frac{dMN}{dt} = k_{t1}MC - k_{t2}MN - V_9C\frac{MN}{K_9+MN} + V_{10}\frac{MNP}{K_{10}+MNP} \quad \text{(S3B)}$$

$$\frac{dMNP}{dt} = V_9C\frac{MN}{K_9+MN} - V_{10}\frac{MNP}{K_{10}+MNP} + k_{t3}MCP - k_{t4}MNP \quad \text{(S3C)}$$

$$\frac{dMCP}{dt} = -k_{t3}MCP + k_{t4}MNP + V_{11}C\frac{MC}{K_{11}+MC} - V_{12}\frac{MCP}{K_{12}+MCP} \quad \text{(S3D)}$$

In these equations, k_{t1}, k_{t2}, k_{t3}, and k_{t4} denote apparent first-order rate constants for transport of the various forms of Msn2 into and out of the nucleus. V_9 and V_{11} denote, respectively, the maximum rates of phosphorylation of the cytosolic and nuclear forms of Msn2 by PKA; V_{10} and V_{12} denote, respectively, the maximum rates of dephosphorylation of the cytosolic and nuclear forms of Msn2 controlled by stress, where

and $V_9 = k_{c9}\mathrm{PKAt}/\mathrm{MSNt}, V_{10} = \mathrm{Str}V_{\max 10}/\mathrm{MSNt}$

$V_{11} = k_{c11}\mathrm{PKAt}/\mathrm{MSNt}, V_{12} = \mathrm{Str}V_{\max 12}/\mathrm{MSNt}.$

The total fractions of Msn2 in the cytosol (M_{cyto}) and in the nucleus (M_{nucl}) are given by the following equation:

$$M_{cyto} = MC + MCP \text{ and } M_{nucl} = MN + MNP. \quad \text{(S4)}$$

The total conservation equation $1 = M_{\mathrm{cyto}} + M_{\mathrm{nucl}}$ allows us to compute one of the four fractions of Msn2 from the three other fractions and to relinquish the corresponding kinetic equation in Equations S3A–S3D.

Parameter Values

The parameter values used in this model, listed in Table S2, were chosen as close as possible to what could be found in the cell. We used the systematic data published by Ghaemmaghami et al. [S4] to estimate the order of magnitude of different components. We took a value of 30 fl for the cellular volume of the haploid cells used in our experiments to calculate their concentration. Thus the concentration of the PKA was set to 0.3 μM. This is an intermediate value between that found for regulatory subunits (Bcy1) and catalytic subunits (Tpk) (Bcy1 = 4300 and Tpk = ±8000 copies per cell). The phosphodiesterase concentration PDE was set to 0.5 μM (sum of Pde1 and Pde2 = ±7500 copies per cell). The concentration of the components localized at the plasma membrane was multiplied by a factor of 250, the estimated ratio between the cellular and the cortex volume, with the assumption of a thickness of 5 to 10 nm for the cortex. Thus, the GEF concentration was set equal to 4 μM for an estimation of 320 copies per cells, whereas the concentration of RAS was set equal to 250 μM for an estimation of 20,000 copies per cell. In the absence of data for GAP (Ira1, Ira2) and for adenylate cyclase, probably because of their lower amount, we estimated these proteins to be approximately 50 molecules per cell, giving final values of 0.7 μM and 1.5 μM for CYCLt and GAPt (Ira1 + Ira2), respectively. As indicated below (Table S3), oscillations occur over a wide range of concentrations of components of the cAMP-PKA system.

We took the kinetic parameters described in the literature, such as the Kd of Cdc25 (GEF) and GAP for Ras [S5], and their kcat measured in vitro for GEF [S6] and NF1 (homolog of Ira1 and Ira2) [S7]. Then, with a concentration of Ras estimated as 250 μM at the membrane, we set the normalized values K_5 and K_6 in the model to 0.001. It is noteworthy that these values fulfill the requirements for zero-order ultrasensitivity [S8] ([Ras]>>Km for GEF and GAP).

In absence of kinetic data on the activation of the adenylate cyclase by Ras in *S. cerevisiae*, we set k_a = 0.01 μM · min^{-1} and $k_i = 1\ \mathrm{min}^{-1}$, assuming a fast process of enzyme activation and inactivation. The catalytic constant for cAMP production was assumed to be close to that found for the homologs of adenylate cyclase in higher eukaryotic cells, in the range of 10 to 20 s^{-1} (600 to 1200 min^{-1}) (http://doqcs.ncbs.res.in/). Taking a value of 1000 min^{-1}, we divided it by 250 to take into account the change of the cellular compartment from the membrane cortex to the cytosol.

The phosphodiesterase of low affinity was reported to be controlled by the feedback [S9]; therefore, we set the K_{md} to 20. The catalytic constant k_d, reported to be quite high, was set to 100 min^{-1}, as estimated from published data [S10]. In the absence of full knowledge on the complex regulation of the PKA [S11], we used a simplified model of PKA activation by cAMP and set the rate constants of activation and inactivation to 1 $\mu\mathrm{M}^{-2} \cdot \mathrm{min}^{-1}$ and 1 min^{-1}, corresponding to fast enzyme activation and inactivation, as suggested in a recent report [S12]. To account for abrupt switches between active and inactive forms of GEF, GAP, and PDE, we used Michaelis-Menten kinetics with V_{max} values varying between 1 min^{-1} and 1.5 min^{-1} and normalized Michaelis constants between 0.01 and 0.05. Because of the phenomenon of zero-order ultrasensitivity [S8], the latter values give rise to sharp thresholds in the activation/inactivation of these components.

To incorporate the coupling of Msn2 to the activity of PKA, we considered a single phosphorylation of Msn2 by PKA, both in the cytosol and in the nucleus. In the absence of precise information on these steps, the normalized Michaelis constants for the kinase and the phosphatase were set equal to 0.05 and the rate of

Table S2. Definition and Numerical Value of the Model Parameters

Kinetic Steps	Parameters	Values	Definition
Activation of GEF			
	GEFt (Cdc25)	4 μM	Total GEF concentration at the membrane
	V_{max1}	1 $\mu M \cdot min^{-1}$	Maximum activation rate
	V_{max2}	1 $\mu M \cdot min^{-1}$	Maximum inactivation rate
	K_1	0.05	Normalized Michaelis constant of activating enzyme
	K_2	0.05	Normalized Michaelis constant of inactivating enzyme
Activation of GAP			
	GAPt (Ira1, Ira2)	1.5 μM	Total GAP concentration at the membrane
	k_{c3}	3.5 min^{-1}	Catalytic constant for activation of GAP by PKA
	V_{max4}	1.3 $\mu M \cdot min^{-1}$	Maximum inactivation rate
	K_3	0.01	Normalized Michaelis constant of activating enzyme
	K_4	0.01	Normalized Michaelis constant of inactivating enzyme
Activation of RAS			
	RASt (Ras1, Ras2)	250 μM	Total RAS concentration at the membrane
	k_{GEF}	240 min^{-1}	Rate constant for GDP to GTP exchange
	k_{GAP}	600 min^{-1}	Rate constant for GTPase activity of RAS
	K_5	0.001	Normalized Michaelis constant of GEFa for RAS-GDP
	K_6	0.001	Normalized Michaelis constant of GAPa for RAS-GTP
Activation of Adenylate Cyclase			
	CYCLt (Cyr1)	0.7 μM	Total adenylate cyclase concentration at the membrane
	k_a	0.01 $\mu M^{-1} \cdot min^{-1}$	Ras-dependent activation rate constant
	k_i	1 min^{-1}	Inactivation rate constant
Production of cAMP			
	k_s	4 min^{-1}	Catalytic constant of adenylate cyclase
Activation of Phosphodiesterase			
	PDEt	0.5 μM	Total phosphodiesterase concentration
	k_{c7}	3.333 min^{-1}	Estimated catalytic constant of PKA acting on PDEi
	V_{Max8}	1.5 $\mu M \cdot min^{-1}$	Maximum inactivation rate
	K_7	0.01	Normalized Michaelis constant of PKA for PDEi
	K_8	0.01	Normalized Michaelis constant of inactivating enzyme for PDEa
Degradation of cAMP			
	k_d	100 min^{-1}	Estimated catalytic constant of PDEa
	K_{md}	20 μM	Normalized Michaelis constant of PDEa
Activation of PKA			
	PKAt (Bcy1, Tpk)	0.3 μM	Cellular concentration of PKA
	a	1 $\mu M^{-2} \cdot min^{-1}$	Rate constant for cAMP-dependent activation of PKA
	r	1 min^{-1}	Rate constant for inactivation of PKA
Phosphorylation and Dephosphorylation of Cytoplasmic Mns2			
	MSNt	1 μM	Total concentration of Msn2
	k_{c9}	3.333 min^{-1}	Estimated catalytic constant for Msn2 phosphorylation by PKA
	V_{Max10}	0.6 $\mu M \cdot min^{-1}$	Estimated maximum rate of Msn2 dephosphorylation
	K_9	0.05	Normalized Michaelis constant
	K_{10}	0.05	Normalized Michaelis constant
Phosphorylation and Dephosphorylation of Nuclear Mns2			
	k_{c11}	3.333 min^{-1}	Estimated catalytic constant of phosphorylation
	V_{Max12}	2 $\mu M \cdot min^{-1}$	Estimated catalytic constant of dephosphorylation
	K_{11}	0.05	Normalized Michaelis constant for Msn2 phosphorylation
	K_{12}	0.05	Normalized Michaelis constant for Msn2 dephosphorylation
Shuttling Parameters of Msn2			
	k_{t1}	10 min^{-1}	Rate constant of import of dephosphorylated Msn2
	k_{t2}	0.001 min^{-1}	Rate constant of export of dephosphorylated Msn2
	k_{t3}	0.001 min^{-1}	Rate constant of import of phosphorylated Msn2
	k_{t4}	10 min^{-1}	Rate constant of export of phosphorylated Msn2

The parameters are grouped according to the kinetic step in which they appear. When they refer to the total concentration of a protein component in the Parameters column, the name of the component is indicated, together with the corresponding yeast gene product in parentheses. The choice of numerical value (the Values column) is justified in the text.

Table S3. Range of Concentrations the cAMP-PKA Components Allowing Sustained Oscillations in the Model

Component	Basal Value Considered in the Model (μM) (see Table S2)	Minimal value (μM)	Maximal Value (μM)
GEFt	4	0.41	7.14
RASt	250	2.1	1429
GAPt	1.5	0.85	20.19
CYCLt	0.7	0.02	4.93
PDEt	0.5	0.23	18.3
PKAt	0.3	0.19	2.38

The concentration of each component was varied in the model, one at a time, from a minimal to a maximal value, giving rise to sustained oscillations of cAMP. Other parameters were held at the values indicated in Table S2. The data were obtained by numerical integration of the kinetic Equations S1A– S1G with the Berkeley Madonna program.

dephosphorylation was adjusted to 2 $\mu M \cdot min^{-1}$ in the cytoplasm and 0.6 $\mu M \cdot min^{-1}$ in the nucleus.

The rates of import and export of Msn2 were chosen so as to reproduce the kinetics of these processes observed experimentally. Thus k_{t1} and k_{t4} were set equal to 10 min^{-1}. This value is compatible with recent measurements made with different cargos and showing that the rate limiting factor for import is the concentration of karyopherins [S13]. The remaining rate constants for import and export, k_{t2} and k_{t3}, were considered as corresponding to negligible reactions and were given a value of 0.001 min^{-1}.

Role of Multiple Negative-Feedback Loops and Zero-Order Ultrasensitivity in the Onset of cAMP Oscillations

In the model, two negative-feedback loops involving PKA control cAMP accumulation. One feedback is exerted on GAP, and the second is exerted on PDE. Oscillations can already occur in the presence of a single feedback loop acting on GAP. One effect of the feedback loop acting on PDE is to lower the minimum of cAMP between two peaks and, hence, to increase the amplitude of cAMP and Msn2 oscillations.

In the RAS module, zero-order ultrasensitivity, which occurs when GEF and GAP are saturated by RAS, favors the onset of oscillations. Such ultrasensitivity, however, is not a prerequisite for sustained oscillations because negative feedback on PDE provides an additional source of periodic behavior.

Irregular Nature of Msn2 Oscillations

The irregular nature of the nucleocytoplasmic oscillations of Msn2 within a single yeast cell can have multiple causes. One is the occurrence of stochastic fluctuations that are due to the relatively small number of molecules observed for at least some components of the cAMP-PKA-Msn2 system. Stochastic models for circadian rhythms show how circadian oscillations become increasingly irregular as the number of mRNA and proteins involved in the clock mechanism progressively diminishes [S14, S15]. As shown experimentally in yeast [S16, S17], stochasticity may further arise because of the random transitions between the on and off states of promoters.

Complex Oscillatory Phenomena

Besides simple periodic oscillations, we have observed in the model various modes of complex oscillatory behavior which will be studied in detail elsewhere. Among these complex oscillatory phenomena are the coexistence of a stable steady state and a stable oscillatory regime, complex periodic oscillations in the form of bursting, and chaos. We have also observed the coexistence of two stable periodic regimes and a stable steady state. In contrast to the simple periodic oscillations considered here, these complex modes of oscillatory behavior occur in a restricted range of parameter values.

Supplemental References

S1. Seedorf, M., and Silver, P.A. (1997). Importin/karyopherin protein family members required for mRNA export from the nucleus. Proc. Natl. Acad. Sci. USA *94*, 8590–8595.

S2. Gorner, W., Durchschlag, E., Martinez-Pastor, M.T., Estruch, F., Ammerer, G., Hamilton, B., Ruis, H., and Schuller, C. (1998). Nuclear localization of the C2H2 zinc finger protein Msn2p is regulated by stress and protein kinase A activity. Genes Dev. *12*, 586–597.

S3. Jacquet, M., Renault, G., Lallet, S., De Mey, J., and Goldbeter, A. (2003). Oscillatory nucleocytoplasmic shuttling of the general stress response transcriptional activators Msn2 and Msn4 in Saccharomyces cerevisiae. J. Cell Biol. *161*, 497–505.

Table S4. Range of Variation of Parameters of the cAMP-PKA Pathway Allowing Sustained Oscillations in the Model

Parameter	Basal Value Considered in the Model (see Table S1)	Minimal Value	Maximal Value
K_1	0.05	0.006	0.945
K_2	0.05	0.003	0.417
K_3	0.01	<0.001	0.125
K_4	0.01	<0.001	0.062
K_5	0.001	<0.001	8.5
K_6	0.001	<0.0001	0.0023
K_7	0.01	<0.001	0.21
K_8	0.01	<0.006	>100
K_{md}	20	0.11	42.6
k_{GEF} (min^{-1})	240	25	427
k_{GAP} (min^{-1})	600	337	>3000
k_a ($\mu M^{-1} \cdot min^{-1}$)	0.01	<0.001	0.025
k_i (min^{-1})	1	0.4	123
k_s (min^{-1})	4	0.11	28.17
k_d (min^{-1})	100	47.4	>3000
a ($\mu M^{-2} \cdot min^{-1}$)	1	<0.001	10.70
r (min^{-1})	1	0.092	>3000
k_{c3} (min^{-1})	3.5	2.75	4.05
k_{c7} (min^{-1})	3.333	2.763	>3000

The values of each parameter were varied in the model, one at a time, from a minimal to a maximal value, giving rise to sustained oscillations of cAMP. Other parameters were held at the values indicated in Table S2. The data were obtained by numerical integration of the kinetic Equations S1A–S1G with the Berkeley Madonna program.

S4. Ghaemmaghami, S., Huh, W.K., Bower, K., Howson, R.W., Belle, A., Dephoure, N., O'Shea, E.K., and Weissman, J.S. (2003). Global analysis of protein expression in yeast. Nature *425*, 737–741.

S5. Haney, S.A., and Broach, J.R. (1994). Cdc25p, the guanine nucleotide exchange factor for the Ras proteins of Saccharomyces cerevisiae, promotes exchange by stabilizing Ras in a nucleotide-free state. J. Biol. Chem. *269*, 16541–16548.

S6. Lenzen, C., Cool, R.H., Prinz, H., Kuhlmann, J., and Wittinghofer, A. (1998). Kinetic analysis by fluorescence of the interaction between Ras and the catalytic domain of the guanine nucleotide exchange factor Cdc25Mm. Biochemistry *37*, 7420–7430.

S7. Ahmadian, M.R., Hoffmann, U., Goody, R.S., and Wittinghofer, A. (1997). Individual rate constants for the interaction of Ras proteins with GTPase-activating proteins determined by fluorescence spectroscopy. Biochemistry *36*, 4535–4541.

S8. Goldbeter, A., and Koshland, D.E., Jr. (1981). An amplified sensitivity arising from covalent modification in biological systems. Proc. Natl. Acad. Sci. USA *78*, 6840–6844.

S9. Ma, P., Wera, S., Van Dijck, P., and Thevelein, J.M. (1999). The *PDE1*-encoded low-affinity phosphodiesterase in the yeast Saccharomyces cerevisiae has a specific function in controlling agonist-induced cAMP signaling. Mol. Biol. Cell *10*, 91–104.

S10. Londesborough, J., and Lukkari, T.M. (1980). The pH and temperature dependence of the activity of the high Km cyclic nucleotide phosphodiesterase of bakers' yeast. J. Biol. Chem. *255*, 9262–9267.

S11. Vigil, D., Blumenthal, D.K., Brown, S., Taylor, S.S., and Trewhella, J. (2004). Differential effects of substrate on type I and type II PKA holoenzyme dissociation. Biochemistry *43*, 5629–5636.

S12. Portela, P., Howell, S., Moreno, S., and Rossi, S. (2002). In vivo and in vitro phosphorylation of two isoforms of yeast pyruvate kinase by protein kinase A. J. Biol. Chem. *277*, 30477–30487.

S13. Timney, B.L., Tetenbaum-Novatt, J., Agate, D.S., Williams, R., Zhang, W., Chait, B.T., and Rout, M.P. (2006). Simple kinetic relationships and nonspecific competition govern nuclear import rates in vivo. J. Cell Biol. *175*, 579–593.

S14. Barkai, N., and Leibler, S. (2000). Circadian clocks limited by noise. Nature *403*, 267–268.

S15. Gonze, D., Halloy, J., and Goldbeter, A. (2002). Robustness of circadian rhythms with respect to molecular noise. Proc. Natl. Acad. Sci. USA *99*, 673–678.

S16. Becskei, A., Kaufmann, B.B., and van Oudenaarden, A. (2005). Contributions of low molecule number and chromosomal positioning to stochastic gene expression. Nat. Genet. *37*, 937–944.

S17. Blake, W.J., Balazsi, G., Kohanski, M.A., Isaacs, F.J., Murphy, K.F., Kuang, Y., Cantor, C.R., Walt, D.R., and Collins, J.J. (2006). Phenotypic consequences of promoter-mediated transcriptional noise. Mol. Cell *24*, 853–865.